TECHNICAL UNIVERSITY OF CLUJ-NAPOCA

ACTA TECHNICA NAPOCENSIS

Series: Applied Mathematics, Mechanics, and Engineering
Vol. 68, Issue II, June, 2025

MICROSTRUCTURAL AND MECHANICAL ANALYSIS OF SHEET METAL BLANKING

Mounir TRABELSI, Boutheina BEN FRAJ, Hamdi HENTATI, Taoufik KAMOUN, Mohamed HADDAR

Abstract: *The blanking test is performed under a variety of process parameters at various levels. Uncontrolled burr (Hbv) and the maximum blanking force (F_{max}) is measured to predict the fracture mechanisms and to design tools. In this paper, design of experiments (DOE) and machine-learning (ML) methods were developed in order to predict Hbv and F_{max} in blanking test. Hbv and F_{max} are affected principally by the sheet thickness. Then, microstructural behavior is experimentally analyzed as function of sheet thickness. After that, series of experiment-based data into ML models training are elaborated to predict Hbv and Fmax. The proposed ML models, Random Forest (RF) and XGBoost (XGB), offer the best prediction of the output parameters.*

Key words: *Metal blanking, Microstructural analysis, Design of Experiments, Machine-learning models.*

1. INTRODUCTION

Various studies have been conducted to predict the damage progression in engineering components subjected to diverse loading conditions [1,2]. These investigations contribute significantly to understanding how material behavior depends on manufacturing parameters, thereby enhancing the durability and efficiency of manufacturing equipment. In this context, design of experiments (DOE) and machine-learning (ML) techniques are considered as appreciated tools to determine the main factors that affected outcomes. In fact, Ben Fraj et al. [3] proved the efficiency of the DOE method to predict outcomes in sheet forming process. Outeiro et al. [4] used the DOE to explore how cutting conditions affects outcomes such as forces and residual stresses. Preez et al. [5] have presented the application of various ML methods within cutting processes and analyzed their efficiency. Ammar et al. [6] used a full factorial as DOE method to determine the mechanical properties of printed composites.

The sheet cutting is an essential operation that precedes many sheet metal working processes. The blanking process is considered as one of the most used techniques in sheet cutting processes [7]. In this context, few studies were developed in order to optimize blanking parameters [8-10]. They used predictive finite element modeling and experimental cutting tests with neural networks to analyze effectively blanking parameters. While blanking processes have seen notable technological improvements, the development of robust models is still limited. It was reported that many factors affect blanking process, which leads to variations in its output parameters [11,12].

Experimental analyses are developed in order to study the influence of the clearance, the friction and the cutting parameters on the obtained geometrical quality and the growth of the burr at the sheet edge [13,14]. Other researchers focus on the influence of blanking parameters on the wear of the punch [15,16].

The main purpose of this paper is to determine the main factors that affect the maximum blanking force (F_{max}) and the blanking burr (Hbv). For various selected levels, these factors are the sheet thickness of part, the punch radius, the punch speed and the clearance between punch and die. The experiment results were validated by a microstructural characterization.

Received: 30.04.25; **Similarities**: 29.05.25: **Reviewed**: 06.06./12.06.25: **Accepted**:19.06.25.

A series of experimental data is used to train ML models for predicting the blanking outcomes.

2. EXPERIMENTAL METHODS AND RESULTS

2.1 Experiments and methods

Blanking tests involve applying punch and die pressure to sheet metal. Currently, suitable parameters for a new product are identified through multiple experimental trials. The material used in this study is S235 steel. Sheets with different thicknesses are examined. The mechanical behavior of the tested steel is investigated using blanking test.

The experiments utilize a specialized blanking tool. A universal tensile machine is used to conduct the blanking tests at various cutting speeds, at room temperature (Fig. 1(a)). The experimental procedure involves placing the workpiece on the die and applying pressure through the descending punch until damage occurs. Fig. 1(b) displays the 3D design of the specific blanking tool employed for cutting metal sheets.

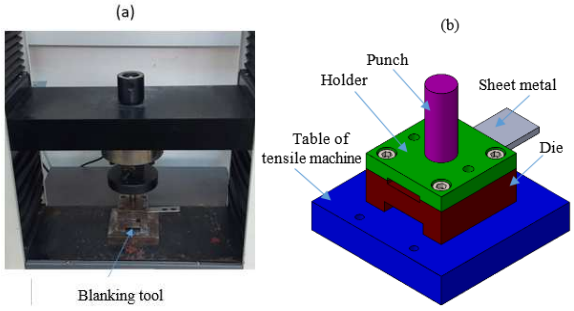

Fig. 1. (a) Blanking trial and (b) 3D scheme of tools

Previous experimental studies in cutting process identify the factors that affect the blanking force and the cut part profile. It was found that the obtained results are affected by sheet thickness and tools geometry such as clearance and punch diameter [17,18]. Accordingly, the effects of sheet thickness (Th), punch diameter (D_p), punch speed (S_p) and clearance (Cl) on the maximum force (F_{max}) and blanking burr (Hbv). The clearance is expressed by:

$$Cl(\%) = 100.\frac{D_d - D_p}{2\,.\,Th}. \qquad (1)$$

Where D_d is the die diameter. In order to identify the material microstructure, the X-Ray Diffraction (XRD) analysis was performed, at the ambient temperature, using a D8 Advance diffractometer with Cu Kα radiation (λCu = 1.54 Å). The XRD samples are the S235 blanks with different thicknesses, 1mm and 2mm, and 14mm of punch diameter. The same punch speed and clearance are applied to obtain these two specimens. The diffraction configurations are recorded over 2θ ranging from [20°,100°], during 30 minutes, by continuous scan with tube voltage of 40 kV and tube current of 40 mA.

2.2 Experimental results of sheet blanking test

To avoid the scrap from twisting or getting wedged between the die and the punch, the strip layout must consider the distance between the blanks and the strip edge, as well as the spacing between adjacent blanks.

The input parameter values for blanking tests are detailed in Table 1.

Table 1

Input factors in blanking tests

S_p (mm/min)	20 - 25 - 30 - 40
D_p (mm)	12 - 14 - 18
Cl (%)	10 - 15 - 20 - 25
Th (mm)	1 - 1.5 - 2

We selected 43 combinations of these input parameters. To ensure result reproducibility, each experiment was conducted twice, resulting in a total 86 blanking tests. Table 2 lists samples of obtained experimental results.

Table 2

Samples of experimental results

S_p (mm/min)	Cl (%)	Th (mm)	D_p (mm)	Hbv (mm)	F_{max} (kN)
40	20	1	14	0.26	13.677
20	15	1.5	12	0.15	17.513
20	10	2	14	0.83	31.39
25	20	1.5	12	0.17	18.103
20	20	2	18	0.75	43.358
20	15	1	12	0.34	10.473
30	15	1	12	0.23	10.593
25	25	2	12	0.42	24.073
20	20	1	18	0.25	18.207
20	15	2	12	0.44	23.46

The result of each blanking test is represented by using a load–displacement curve that represents the punch movement. The maximum force (F_{max}) is determined from the following

curve (Fig. 2) for Th = 1 mm, D_p = 14 mm, S_p = 40mm/min and Cl = 20%.

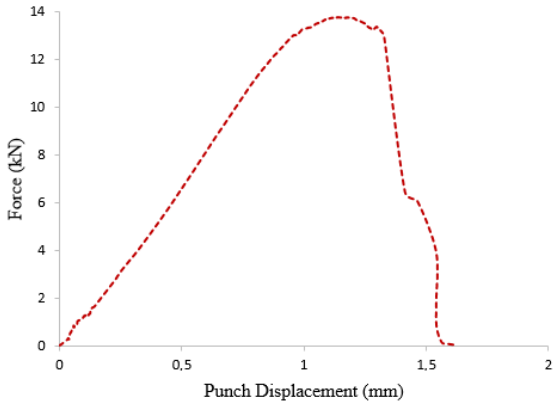

Fig. 2. Experimental F_{max} (Th = 1 mm, Dp = 14 mm, Sp = 40 mm/min and Cl = 20%)

As illustrated in Fig. 2, the blanking process comprises three distinct phases delineated by the load–displacement curve. The initial punch phase involves the punch affecting the sheet metal, initiating elastic deformation. If stresses surpass the material's maximum shear strength, plastic deformation occurs. When the shearing stress exceeds the material's fracture threshold, tearing occurs and the stored elastic energy is suddenly released. In the subsequent push phase, the sheet part is entirely expelled from the die, with the punch traversing of the bottom dead center. Finally, in the withdrawal phase, as the punch is extracted from the die, withdrawal forces arise due to the interaction between the sheet and the punch causing jamming.

Fig. 3 shows blanking burrs, which can be prevented by analyzing the influence of key parameters throughout the design and manufacturing stages of the blanking process.

Fig. 3. Blanking burr during cutting operation

3. DESIGN OF EXPERIMENTS RESULTS FOR BLANKING PROCESS

DOE method is employed to investigate the correlation between various input factors and the outcomes of the blanking process, specifically focusing on F_{max} and Hbv. The main objective is to facilitate a precise estimation of the influence of each factor of the blanking process and to understand their impacts on F_{max} and Hbv evolutions.

In order to establish a mathematical model for F_{max} and Hbv, we chose to use a full factorial design in which the output results are determined for all combinations of factor levels. Indeed, two levels for each input have been selected. At each level (i), the sheet thickness, the punch diameter, the punch speed and the clearance are denoted Th-i, D_p-i, S_p-i, and Cl-i, respectively. The values of the process factors at different levels are presented in Table 3.

Table 3

Input factors for DOE analysis

Factors	Level	Value
Th-1 (mm)	1	1
Th-2 (mm)	2	2
D_p-*1* (mm)	1	14
D_p-*2* (mm)	2	16
S_p-*1* (mm/min)	1	20
S_p-*2* (mm/min)	2	40
Cl-1 (%)	1	10
Cl-2 (%)	2	15

The total number of tests is 16. Each experiment was conducted twice, resulting in a total 32 blanking tests. For each input factor (fact) in level (i), denoted (fact-i), the average of each output parameter (F_{max}) and (Hbv), represented by (X), is calculated as follows:

$$average\,(X) = \sum_{p=1}^{N_t} X_{,p}(fact\text{–}i)\,. \quad (2)$$

Where N_t is the number of the performed tests for each (fact-i). The range between the highest and lowest levels of the average (X) is expressed as follows:

$$\delta(X) = \frac{\text{Max}\,(average\,(X)) - \text{Min}\,(average\,(X))}{2}. \quad (3)$$

3.1 Predictive modeling of maximum blanking force

Accurate prediction of fracture mechanisms in sheet metal and the effective design of blanking tools require a clear understanding of force evolution during the blanking process. The maximum blanking force (F_{max}) depends on various factors, principally the punch speed, sheet metal thickness, the clearance between die and punch, etc. The variation of the average of F_{max} as function of input factors is presented in Fig. 4.

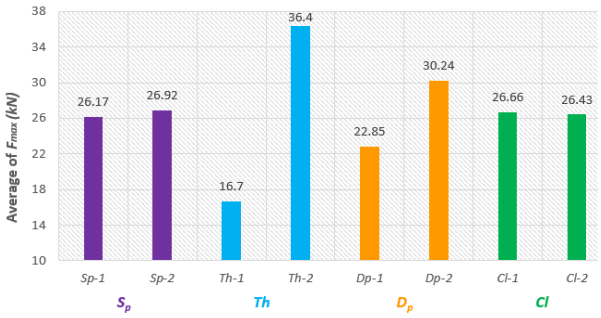

Fig. 4. Variation of the average of F_{max}

Examining the data presented in Fig. 4, it is showed that as the thickness (*Th*) and the punch diameter (D_p) are increased, there is a significant rise in the maximum force (F_{max}). This result indicates a strong effect of these factors on F_{max} evolution. In contrast, the impact of the punch speed (S_p) and the clearance (*Cl*) appears to be comparatively negligible, suggesting that variations in these parameters have a minor effect on Fmax evolution. Emphasizing the design of experiments, an analytical model of the maximum blanking force (F_{max}) is proposed. The first order polynomial model is developed and given by Eq. 4.

$$F_{\max} = 21123.69 + 37.58\ S_p - 1163.78\ Th - 1348.97\ D_p - 7423.75\ Cl + 57.37\ D_p.Cl + 178.12\ Th.Cl + 1557.06\ D_p.Th \quad . (4)$$

We show in Fig. 5, the comparison between the theoretical (F_{max}-*th*), calculated by Eq. 4, and the experimental (F_{max}-*exp*) results of the maximum blanking force.

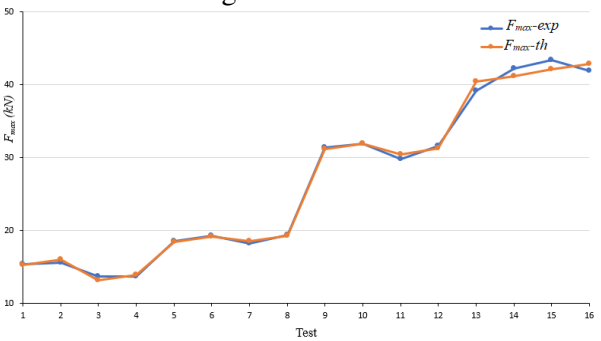

Fig. 5. Validation of mathematical model of F_{max}

3.2 Predictive modeling of blanking burr

Blanking burr is a phenomenon that allows the control of quality in blanking process. It is crucial to control aspects of the blanking operation leading the burr appearance. For that, we measure the burr *Hbv* as function of the selected factors (Table 3). The influence of each factor on *Hbv* will be studied. Fig. 6 illustrates how the average *Hbv* varies with respect to the input factors.

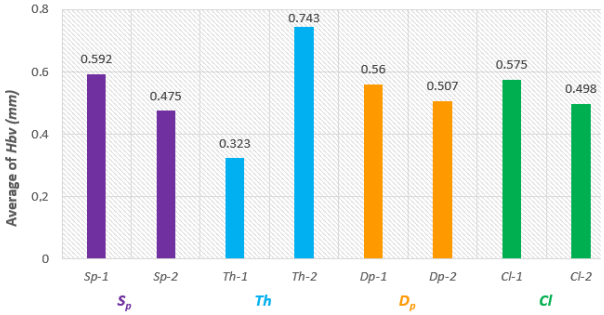

Fig. 6. Variation of the average of *Hbv* with respect to the input factors

From this graph, D_p, S_p, and *Cl* affect moderately the average of *Hbv*. Otherwise, the growth of *Th* significantly increases *Hbv*.

A first order polynomial relation (Eq. 5) contains eleven unknown parameters are used to define the effect of each input factors and their interaction on *Hbv*.

$$Hbv = 561.875\ 10^{-3} - 1.8125\ 10^{-3}\ S_p - 8.125\ 10^{-3}\ Cl - 27.1875\ 10^{-3}\ D_p + 291.25\ 10^{-3}\ Th - 4\ 10^{-3}\ S_p.Th + 0.0625\ 10^{-3}\ S_p.D_p + 0.0625\ 10^{-3}\ S_p.Cl + 12.5\ 10^{-3}\ Th.D_p + 3.25\ 10^{-3}\ Th.Cl - 0.4375\ 10^{-3}\ D_p.Cl \quad . (5)$$

In addition, analytical workpiece burr (*Hbv-th*) is determined by the theoretical model (Eq. (6)) and compared, in Fig. 7, with those which were experimentally measured (*Hbv-exp*).

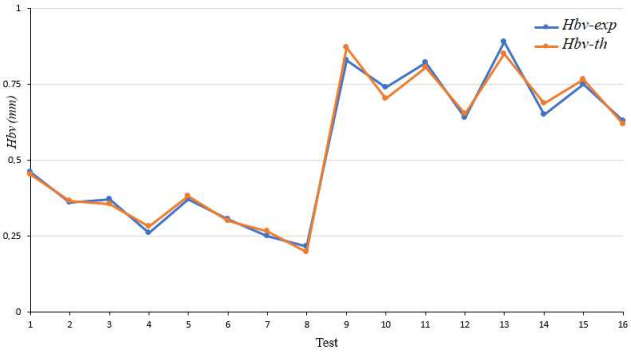

Fig. 7. Validation of theoretical model of *Hbv*

The agreement between measured and predicted values of blanking burr reveals that the developed model (Eq. 4) offers a good estimation of this parameter.

3.2 Synthesis

To verify the reliability of the theoretical models for *Hbv-th* and F_{max}*-th*, a comparison is made using supplementary tests that were not part of the initial blanking experiments. In this context, other experiment blanking tests were performed (Table 4).

Table 4

Blanking experimental tests for validation

S_p (mm/min)	*Cl* (%)	*Th* (mm)	D_p (mm)	*Hbv* (mm)	F_{max} (kN)
20	15	1	12	0.34	10.473
25	25	1	12	0.16	10.66
30	25	1	12	0.15	10.633
30	20	1.5	12	0.24	18.22
30	25	1.5	12	0.22	17.993
25	25	2	12	0.42	24.073

Based on Table 4, a comparison between analytical, based on DOE nanlysis and experimental results is conducted as follow (Figs. 8 and 9).

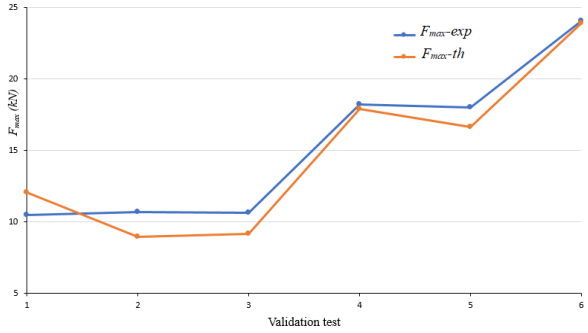

Fig. 8. Accuracy of mathematical model of F_{max}

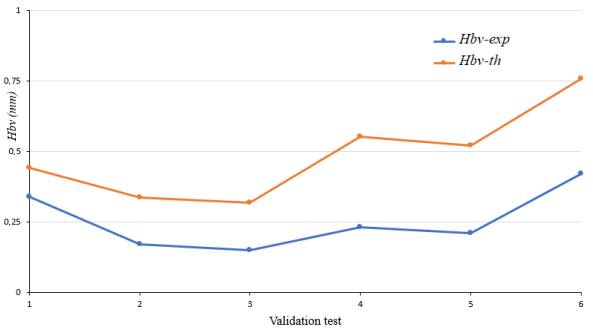

Fig. 9. Accuracy of mathematical model of *Hbv*

When input parameters, not considered in the development of the analytical model, are changed, errors increase, especially in the prediction of *Hbv*. The analytical model is not effective in predicting F_{max} and *Hbv* when an input parameter takes a value different from those taken in the experimental design.

4. MICROSTRUCTURAL ANALYSIS

It was proved, in section 3, that the sheet thickness is the most influent among the selected input factors since it has a great influence on both *Hbv* and F_{max}. For this reason, the microstructural characterization of the punched parts is performed to investigate the effect of the sheet thickness on the microstructural behavior of S235 under blanking test. XRD pattern of the obtained parts is presented in Fig. 10 as function of the thickness.

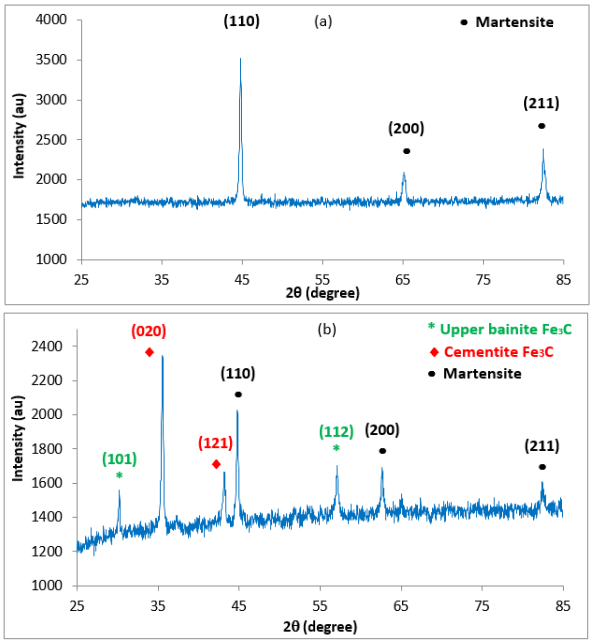

Fig. 10. XRD analysis of punched S235 steel at two specimen thicknesses: (a) 1 mm and (b) 2 mm

Fig. 10 shows that the martensite phase characterizes the microstructure of the thinnest specimen. Three characteristic peaks were revealed in Fig. 10(a). Nevertheless, for the specimen which having 2mm of thickness, the S235 behaves differently from microstructural point of view Fig. 10(b). In addition to martensitic peaks, a strong and narrow diffraction peak was exhibited at 2θ equal to 35.54° and indexed to (020) crystallographic plane of cementite (Fe3C) with another peak indicating the same phase at 43.16°. The weaker diffraction peaks at 30.2° and 57.11°, corresponding respectively to (101) and (112) crystallographic planes, show the presence of a third phase in the material microstructure which is the upper bainite (Fe3C). The volume

fractions of the detected phases are mentioned in Fig. 11.

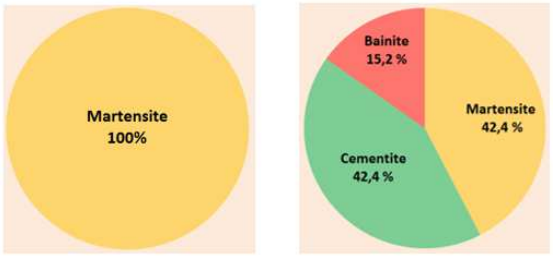

Fig. 11. Volume fractions of cementite, martensite and bainite phases in the punched parts microstructure: (a) 1mm; (b) 2mm

The obtained XRD pattern was compared with that of the unpunched one [19] as well as with that of the low carbon steel (0.2% C) [20] (Fig. 12).

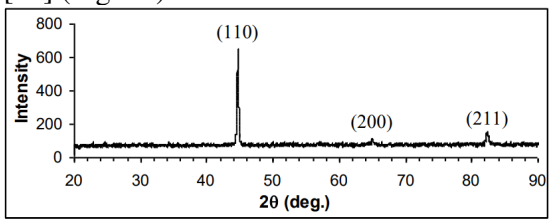

Fig. 12. XRD pattern of low carbon steel (Ferritic microstructure) [20]

It can be concluded that the blanking test has a great effect on the microstructural behavior of this metal. As cast, before blanking test, the S235 XRD pattern exhibits ferrite phase as the initial phase [19]. The XRD analyses, in Fig. 10, indicate that a stress induced phase transformation takes place during the blanking test, which, depends on the specimen thickness. Regarding the thickness of 2 mm, the appearance of bainite and cementite phases in Fig. 10(b) can be attributed to the presence of thermal effect due to a thermo-mechanical phase transformation or to an eventual internal frictional energy.

To improve the understanding of this result, the microstrain and the crystallite size of the punched S235 steel, with the two thickness levels, were determined for each peak. The averages of these microstructural parameters are summarized and inserted in Table 8.

- The Full Width at Half Maximum (FWHM), denoted as β, represents the width of a diffraction peak measured at 50% of its maximum intensity. It is used to characterize different material properties. It must be converted into radians in the following calculation.

- D is the crystallite size, expressed by Scherrer's equation:

$$D = \frac{K\ \lambda}{\beta\ \cos(\theta)}. \quad (6)$$

K is the shape factor (K = 0.94) and λ is the X-ray wavelength (λ = 1.54 Å).

- ε is the microstrain which was determined by:

$$\varepsilon = \frac{\beta}{4\ \tan(\theta)}. \quad (7)$$

Microstrains are often attributed to the presence of the dislocations already created during the blanking test. The dislocation density can be influenced by the selected input factors as the punch speed, thickness and punch diameter; and can be able, simultaneously, to influence F_{max} and *Hbv*. From the determined parameters, the dislocation density (δ) may be determined by the following relationship (Eq. (8)).

$$\delta = \frac{1}{D_a^{\ 2}}. \quad (8)$$

Where D_a is the average crystallite size.

Table 5

Variation of microstrain, crystallite size, and dislocation density with sheet thickness in punched parts.

	Average microstrain ε_a (x10^{-3})	Average crystallite size D_a (nm)	Dislocation density δ (x10^{-3} nm^{-2})
Th-1= 1 mm	6.69	11.57	7.47
Th-2 = 2 mm	2.28	40.27	0.61

The obtained results from Table 5 confirm that the increase of specimen thickness, from 1mm to 2mm, is followed, under blanking test, by a great increase of crystallite size and also a considerable decrease of both microstrain and dislocation density which improves the ductile behavior of the tested material. These findings defend and explain the observed thickness effect on F_{max} and *Hbv*.

5. OPTIMIZATION METHOD USING MACHINE-LEARNING MODELS

In recent years, the field of optimizing manufacturing processes has witnessed a remarkable transformation fueled by advancements in machine-learning (ML) technologies. As researchers strive to unravel the complex relationships governing manufacturing parameters, the integration of ML techniques has developed as a great tool for accelerating discovery and optimizing manufacturing process. In this study, we concentrate on the application of ML models for regression tasks, specifically aiming to predict F_{max} and *Hbv*. We explore and compare the efficacy of four regression ML models in this context: XGBoost regression (XGB), Random Forest regression (RF), Support Vector Regression (SVR), and Artificial Neural Network regression (ANN). The Root Mean Squared Error (RMSE) is calculated (Eq. 9) to assess the accuracy of each ML model.

$$RMSE = \sqrt{\frac{1}{N}\sum_{j=1}^{N}\left(y_j - \hat{y}_j\right)^2} \quad . (9)$$

Where N is the number of observations, y_j is the actual value of observation j and $\hat{y}_j$ is the model's prediction for observation j.

5.1 Predicted F_{max}

The *RMSE(%)* is calculated for each ML model in order to predict F_{max} in the blanking process. The obtained results are presented in Fig. 13. Given the low *RMSE(%)* observed in the XGB and RF models, it is evident that these models outperform the ANN and SVR models in terms of predictive accuracy.

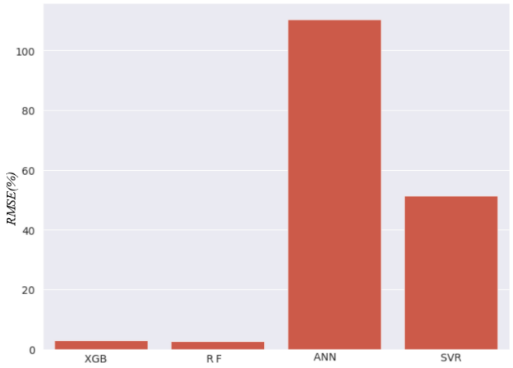

Fig. 13. *RMSE(%)* for each ML model

The XGB and RF models are more reliable in predicting F_{max} with outliers. The predicted results (test dataset) of RF and XGB models are showed in Fig. 14.

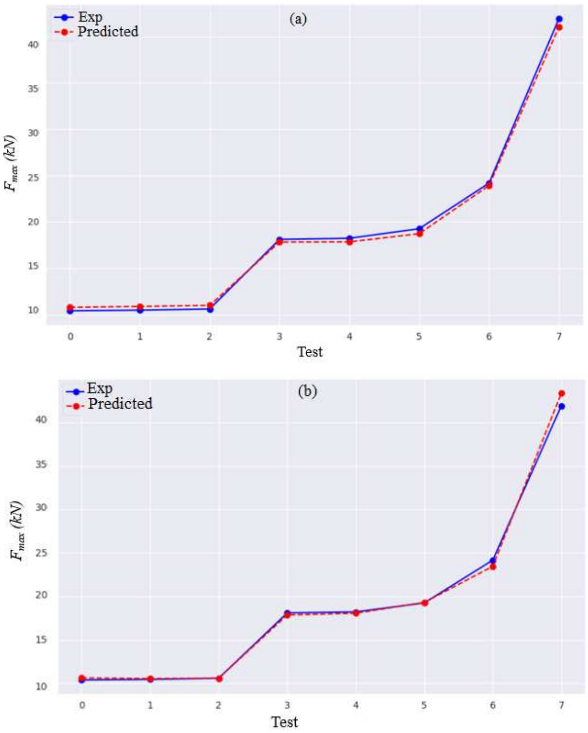

Fig. 14. Predicted F_{max} with two models (a) RF ; (b) XGB

RF and XGB models are deemed as suitable choices, underscoring their reliability and effectiveness in predicting F_{max} in the blanking process.

5.2 Predicted *Hbv*

We delve into the analysis of predicted *Hbv* values. For every ML model, we compute the *RMSE(%)*. Figure 15 presents the outcomes derived from this analysis.

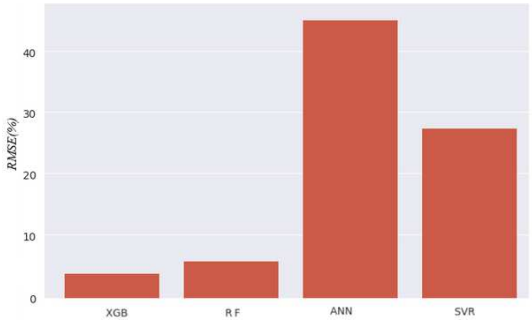

Fig. 15. *RMSE(%)* for each ML model

The XGB and RF models exhibited notably low *RMSE(%)* values, showcasing their strong

predictive capabilities. Interestingly, RF outperformed XGB in terms of predictive accuracy. Conversely, the ANN and SVR models showed considerably higher *RMSE(%)* scores, indicating inferior performance. The predicted results of the following models, RF and XGB, are illustrated in Fig. 16.

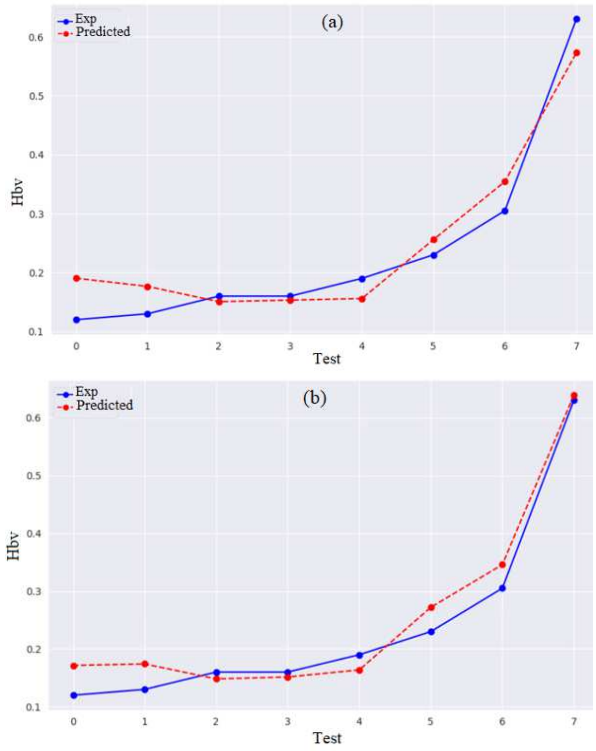

Fig. 16. Predicted *Hbv* (a) RF model ; (b) XGB model

These models are more reliable in predicting *Hbv* with outliers. In fact, XGB and RF are the best ML models used for regression tasks and provide robust predictions.

5. CONCLUSION

Design of experiments method determines the necessary data that contribute significantly and the interaction between different variables with a minimum number of experiments. This study aims primarily to examine how various experimental parameters influence the workpiece burr height (*Hbv*) and the maximum blanking force (F_{max}). The investigated input variables, which are punch speed, punch diameter, clearance between die and punch, and sheet thickness, were identified as key factors affecting these two output responses. New analytical models were proposed and developed in order to support analytical and experimental findings. From the obtained results, it was proved that thickness has a great influence on F_{max} while for Hbv. Then, XRD analysis of the punched parts was conducted to examine the impact of sheet thickness on the microstructural behavior of S235 during the blanking test. In addition, ML models were implemented to predict Hbv and Fmax in the blanking process. A good prediction of Fmax is achieved through the DOE method and RF and XGB models. However, *Hbv* is not well predicted by the DOE method. Conversely, RF and XGB models yield good results.

6. REFERENCES

[1] Hammami, C., Kammoun, N., Hentati, H., Amar, M B., Haddar, M.. *Parametric analysis of the damage characterization tests of aluminum bulk material*, J. Mech. Sci. Technol. 2022, 36: 5019–5025, DOI10.1007/s12206-022-0914-z.

[2]Hentati, H., Dhahri, M., Dammak, F.. *A phase-field model of quasistatic and dynamic brittle fracture using a staggered algorithm.* J Mech Mater Struct 2016, 11: 309–327. DOI: 10.2140/jomms.2016.11.309

[3] Ben Fraj, B., Kamoun, T., Hentati, H., Trabelsi, M., Ghazouani, N., and Ahmed, M. *Optimization of forming force and Erichsen index using Taguchi design of experiments: Mathematical models and experimental validation.* Proc. Inst. Mech. Eng., Part B 2024, 238(9), 1316-1326. https://doi.org/10.1177/09544054231194107

[4]Outeiro, J., Cheng, W., Chinesta, F., and Ammar, A. *Modelling and Optimization of Machining of Ti-6Al-4V Titanium Alloy Using Machine Learning and Design of Experiments Methods*. J. Manuf. Mater. Process. 2022, 6(3), pp. 58. DOI: https://doi.org/10.3390/jmmp6030058

[5]Preez, A., and Oosthuizen, G.A. *Machine learning in cutting processes as enabler for smart sustainable manufacturing*. Procedia Manuf. 2019, 33, pp. 810-817. DOI: https://doi.org/10.1016/j.promfg.2019.04.102

[6]Ammar, S., Ben Fraj, B., Hentati, H., Saouab, A., Ben Amar, M., Haddar, M. *Mechanical performances of printed carbon fiber-reinforced PLA and PETG composites*. Proceedings of the Institution of Mechanical Engineers, Part L: Journal of Materials: Design and Applications. 2024, 238(8):1488-1499. doi:10.1177/14644207231225761

[7]Lange, K. *Handbook of Metal Forming*, McGraw–Hill 1985, ISBN: 0-07-036285-8.

[8]Hambli, R., and Guerin, F.. *Application of a neural network for optimum clearance prediction in sheet metal blanking processes*. Finite Elem. Anal. Des 2003, 39(11), pp.1039-1052.

[9]Unterberg, M., Niemietz, P., Trauth, D., Wehrle, K., and Bergs, T. *In-situ material classification in sheet-metal blanking using deep convolutional neural networks*. Prod. Eng. Res. Devel. 2019, 13, pp. 743-749. DOI: https://doi.org/10.1007/s11740-019-00928-w

[10] Goijaerts, AM., Govaert, LE., and Baaijens, FPT. *Experimental and numerical investigation on the influence of process speed on the blanking process*. J. Manuf. Sci. Eng. 2002, 124(2), pp. 416-419. DOI: https://doi.org/10.1115/1.1445152.

[11] Moakhar, S., Hentati, H., Barkallah, M., Louati, J., Haddar, M.; Bonk, C., Behrens, BA. *Modeling of the ductile damage-Application for bar shearing*. Mater. Wiss. Werkstofftech. 2019;, 50: 1353–1363. https://doi.org/10.1002/mawe.201800128.

[12] Mihăilesc, N., Iancău, H., Achimaş, G.. *Fine blanking and piercing*, ACTA TECHNICA NAPOCENSIS - Series: Applied Mathematics, Mechanics, and Engineering, 59(1), 2016. ISSN 2393–2988.

[13] Akyürek, F., Yaman, K., and Tekiner, Z.. *An experimental work on tool wear affected by die clearance and punch hardness*. Arab. J. Sci. Eng. 2017, 42, pp. 4683-4692.

[14] Lawanwong, K., and Pumchan, W. *Wear mechanism and ability for recovery of tool steel on blanking die process*. Key Eng. Mater. 2017, 725, pp. 572-577.

[15] Maiti, S., Ambekar, A., Singh, U., Date, P., and *Narasimhan, K. Assessment of influence of some process parameters on sheet metal blanking*. J. Mater. Process. Technol. 2000, 102(1-3), 249-256.

[16] Mucha, J., and Tutak, J. *Analysis of the Influence of Blanking Clearance on the Wear of the Punch, the Change of the Burr Size and the Geometry of the Hook Blanket in the Hardened Steel Sheet*. Materials 2019, 12(8), 1261.

[17] Totre, A., Nishad, R., and Bodke, S. *An overview of factors affecting in blanking processes*. Mater. Sci. Eng. 2013.

[18] Chan, H.Y., and Abdullah, A.B. *Geometrical Defect in Precision Blanking/Punching: A Comprehensive Review on Burr Formation*. Res. J. Appl. Sci. 2014, 9, pp. 1139-1148.

[19] Han, W., Kuepper, K., Hou, P., Akram, W., Eickmeier, H., Hardege, J., Steinhart, M., and Schäfer, H.. *Free-Sustaining Three-Dimensional S235 Steel-Based Porous Electrocatalyst for Highly Efficient and Durable Oxygen Evolution*. ChemSusChem 2018, 11(20), 3661-3671.

[20] Aryanto, D., Sudiro, T., and Wismogroho, A.S.. *Correlations between Structural and Hardness of Fe-50%Al Coating Prepared by Mechanical Alloying. Piston*, J. Techn. Eng. 2018, 1(2).

Analiza microstructurală și mecanică a tăierii blancurilor din tablă metalică

Rezumat. Testul de tăiere este realizat sub o varietate de parametri de proces la diferite niveluri. Bavura necontrolată (Hbv) și forța maximă de tăiere (Fmax) sunt măsurate pentru a prezice mecanismele de fractură și pentru a proiecta uneltele. În această lucrare, metodele de planificare a experimentelor (DOE) și de învățare automată (ML) au fost dezvoltate pentru a prezice Hbv și Fmax în testul de tăiere. Grosimea tablei este factorul cu cea mai mare influență asupra Hbv și Fmax. Apoi, comportamentul microstructural este analizat experimental în funcție de grosimea tablei. Ulterior, o serie de date experimentale sunt utilizate pentru antrenarea modelelor ML în scopul prezicerii lui Hbv și Fmax. Modelele ML propuse, Random Forest (RF) și XGBoost (XGB), oferă cea mai bună predicție a parametrilor de ieșire.

Mounir TRABELSI, Maitre Technologue, Higher Institute of Technological Studies of Sfax, Tunisia, mounir.trabelsi@emp.tn

Boutheina BEN FRAJ, Assistant Professor, Research and Technology Center of Energy Technoparc Borj Cedria, Tunisia, boutheina.benfraj2024@gmail.com

Hamdi HENTATI, Associate Professor, Laboratory of Mechanics Modeling and Production, ENIS, University of Sfax, Tunisia, ESSTHS, University of Sousse, Tunisia, hamdi.hentati@yahoo.fr

Taoufik KAMOUN, Technologist Professor, Higher Institute of Technological Studies of Sfax, Tunisia, taoufikkamoun@yahoo.fr

Mohamed HADDAR, Professor, Laboratory of Mechanics Modeling and Production, ENIS, University of Sfax, he was honored with the prestigious first National Prize for Scientific Research and Technology in 2022, mohamed.haddar2016@gmail.com